Desalination and Water Treatment
www.deswater.com

doi: 10.1080/19443994.2016.1159994

57 (2016) 26211–26221
November

Valorisation of a by-product from the TiO_2 pigment industry for its application in advanced oxidation processes

E. Pulido Melián[a,*], L. Santana Viera[a], E. Otal[b], J.M. Doña Rodríguez[a], Dunia E. Santiago[a], C. Fernández-Pereira[b], O. González Díaz[a], L.F. Vilches[b]

[a]*Centro Instrumental Químico—Físico para el Desarrollo de Investigación Aplicada (CIDIA)—Dpto. de Química, Edificio Central del Parque Científico Tecnológico, Grupo de Fotocatálisis y Espectroscopia Aplicada al Medioambiente (FEAM, Unidad Asociada al CSIC por el Instituto de Ciencias de Materiales de Sevilla), Universidad de Las Palmas de Gran Canaria, Campus Universitario de Tafira, 35017 Las Palmas, Spain, Tel. +34 928457298; emails: elisendapm80@hotmail.com (E. Pulido Melián), laura.santana119@alu.ulpgc.es (L. Santana Viera), jose.dona@ulpgc.es (J.M. Doña Rodríguez), dsantiago@proyinves.ulpgc.es (D.E. Santiago), oscar.gonzalez@ulpgc.es (O. González Díaz)*

[b]*Department of Chemical and Environmental Engineering, School of Engineering (ETSI), University of Seville, Camino de los Descubrimientos s/n, 41092 Seville, Spain, Tel. +34 954559529; email: eotal@us.es (E. Otal), Tel. +34 954481379; email: pereira@us.es (C. Fernández-Pereira), Tel. +34 954487282; email: luisvilches@us.es (L.F. Vilches)*

Received 14 December 2015; Accepted 25 February 2016

ABSTRACT

The aim of this study was to find a recycling use for waste material ($WTiO_2$) that results from the extraction process of TiO_2 from ilmenite in the pigment industry. In view of its high TiO_2 content, the photocatalytic activity of this material was tested in the degradation of humic and fulvic acid substances (HFAs) and showed low levels of photoactivity, as was the case for the commercial photocatalyst Aeroxide TiO_2 P25 (P25). However, due to its high Fe^{3+} content, an important application was observed for $WTiO_2$ as an HFA coagulant and catalyst in Fenton and photo-Fenton processes. A two-stage process of coagulation and photo-Fenton treatment was subsequently designed and conducted at laboratory and small pilot scale. High percentages (above 95%) were obtained in total organic carbon (TOC) removal.

Keywords: TiO_2; Valorisation; AOPs; Photo-Fenton; Humic substances; Waste

1. Introduction

The growing population and industrialisation of the more developed countries is having negative consequences for the environment and is increasing water contamination. However, society is slowly but surely becoming more aware of environmental issues and is now striving to achieve a balance between economic, social and environmental progress as a fundamental pillar of sustainable development. Sustainability programmes involve a number of actions aimed, among others, at the reduction, recycling and reuse of waste.

Titanium dioxide is an important raw material in our industrialised world, used most notably as a white pigment for its optical properties, particularly its brightness and high refractive index (>2.4), as well as its chemical stability. Although some 67% of titanium dioxide is used for the production of paints, varnishes

---

*Corresponding author.

and inks, this material is also present in paper, plastics, cosmetics, textiles and food products. Its toxicity is the subject of much debate and, given its extensive use, numerous studies have been made on this raw material.

In 2006, the International Agency for Research on Cancer (IARC) concluded that while there was evidence that TiO_2 is carcinogenic in laboratory animals, there was no evidence of its carcinogenicity in humans and it was classified in "Group 2B: Possible human carcinogen". The National Institute of Occupational Safety and Health (NIOSH) recommends a maximum exposure of $2.4\ mg\ m^{-3}$ in fine and $0.3\ mg\ m^{-3}$ for ultrafine and nanoparticles to reduce risks to workers, but has not found a link between exposure to respirable TiO_2 and lung cancer in workers in industry.

Ilmenite is the most important raw product in the production of TiO_2 and accounted for about 47% of total market volume in 2011. Ilmenite is a mixture of oxides of iron and titanium, and titanium oxide composition varies for different ilmenite samples, but is generally around 50–55%. The remaining 45% of its composition corresponds to iron oxides, ferric or ferrous, with varying ratios between them depending on the age of the mineral [1]. In the paint industry, the two processes for manufacturing the pigment from ilmenite are known as "via chloride" and "via sulphate". In the "via sulphate" process, ilmenite is reacted with concentrated sulphuric acid at 150–220°C resulting in a solution of titanium and iron sulphate and a solid portion composed of insoluble unreacted ore and undissolved digestion cake (Eqs. (1)–(4)). This solid is called sludge cake and is separated from the solution by decantation and filtration. Around 0.5 g of this sludge is formed per gram of titanium dioxide produced. This residue is generally stabilised and solidified and finally placed in landfills.

$$\text{Ilemenite} + \text{sulphuric acid} \longrightarrow \text{cake} + \text{liquor} \tag{1}$$

$$TiO_2 + 2H_2SO_4 \longrightarrow Ti(SO_4)_2 + 2H_2O \tag{2}$$

$$FeO + H_2SO_4 \longrightarrow FeSO_4 + H_2O \tag{3}$$

$$Fe_2O_3 + 3H_2SO_4 \longrightarrow Fe_2(SO_4)_3 + 3H_2O \tag{4}$$

Due to its high content of TiO_2 and Fe(III), this sludge cake could potentially be applied in water treatment processes, specifically in physical processes such as coagulation–flocculation and chemical processes such as advanced oxidation processes (AOPs).

Traditionally, metal coagulants, iron and aluminium salts, have been among the most commonly used chemical substances in water clarification and BOD and phosphate removal from wastewater. They have the advantage of simultaneously acting as coagulants and flocculants. Their coagulating power comes from the ability to form complex hydrated positively charged species ($Fe(H_2O)_6^{3+}$, $Al(H_2O)_6^{3+}$). AOPs are based on physicochemical processes which involve the generation and use of powerful transitory species, mainly the hydroxyl radical ($HO^{\bullet}$). This radical is highly effective in the oxidation of organic matter because, due to its high oxidising power, it can react 106–1,012 times faster than other alternative oxidants such as O_3.

Humic and fulvic acid substances (HFAs) were the chosen pollutant to study the possible use of this residue in water treatment. These substances comprise a growing percentage of the organic matter present in leachate that results from municipal solid waste accumulation at landfills [2–4]. Leachate is formed as a result of rain water percolating through the waste matter and the decomposition of organic compounds. These extremely harmful compounds are not biodegradable and their complete mineralisation is very complex. For a variety of reasons, including their aesthetically displeasing colour which also impedes the penetration of light required for photosynthesis, the formation of metallic ion complexes and organic compounds and, most importantly, the fact that they act as precursors for the formation of chlorine disinfection by-products such as trihalomethanes and haloacetic acids, the elimination of HFAs from potable water supplies has been and continues to be a very important concern [5].

The aim of the present study is to investigate a recycling use for a waste material from the TiO_2 pigment industry ($WTiO_2$) in the treatment of HFA solutions. Due to its high Fe and TiO_2 content, its potential application was studied in physical treatments of water (coagulation–flocculation), as well as in various AOPs (photocatalysis, Fenton and photo-Fenton). Its activity was compared with reference materials as iron salts and TiO_2-based photocatalysts. The latter include a commercial photocatalyst, Aeroxide TiO_2 P25 (P25), and a home-made photocatalyst, ECT-1073t (ECT) [6], whose activity in some cases has exceeded that of P25 [7].

2. Materials, techniques and procedures

2.1. Materials

The by-product $WTiO_2$ is generated from the concentrated sulphuric acid digestion of ilmenite at 150–220°C, where titanium separates in the form of titanyl sulphate which, after hydrolysis, precipitation and calcination, is transformed into TiO_2. The other catalysts used for comparison purposes were Aeroxide TiO_2 P25 (P25) from Evonik Industries and ECT-1073t (ECT) synthesised by the research group from Las Palmas de Gran Canaria University (Patent Publication Number—WO 2013117778 A1) and which exhibits high activity, in some cases even greater than that of P25 [6,7]. The HFAs, Gepavit Humipol, were supplied by Fertinagro (Teruel, Spain) (total organic matter: 70%, total humic extract: 68%, humic acids = 50% and fulvic acids = 18%). H_2O_2 (30% w/v, Panreac) and $FeCl_3{\cdot}6H_2O$ (96%, Panreac) for comparison purposes were used for the Fenton and photo-Fenton processes. H_2SO_4 (96%, Panreac) and NaOH (97%, Panreac) were used for pH adjustment. All solutions were prepared using pure Milli-Q water.

2.2. Analytical determinations

Mineralisation of organic matter was followed by measuring the total organic carbon (TOC) by direct injection of samples into a Shimadzu TOC-VCSH analyser with an NDIR detector, calibrated with standard solutions of potassium phthalate.

Fe concentration lixiviated from the by-product $WTiO_2$ was measured by means of atomic absorption spectrophotometry (AAS) with a SpectrAA with Zeeman background correction from Varian by electrothermal atomisation in a graphite furnace.

The UV–vis absorption spectra were recorded with a UV–visible Heλios Thermo (200–900 nm) spectrophotometer.

pH measurements were carried out using a Crison GLP 21 pH-meter.

The titanium oxalate method was used for H_2O_2 determination. This is based on the reaction of hydrogen peroxide with potassium titanium oxalate ($K_2TiO[C_2O_4]{\cdot}H_2O$) in acid solution to form the yellow pertitanic acid complex which was spectrophotometrically measured at 400 nm [8].

Sample toxicity was determined using the MultiTox® *Vibrio fischeri* toxicity test. This bioassay was performed following standard UNE-EN-ISO 11348-3: 1998, which describes the determination of the inhibitory effect of water samples on the light emission of *V. fischeri* (luminescent bacteria test). Toxicity levels were determined by monitoring the fall in luminescence as a result of the inhibition of bacterial luciferase upon contact with toxic substances. An Optocomp I luminometer from MGM Instruments was used for these measurements.

SEM analysis was carried out using a Hitachi S-4800 microscope. Analysis of elemental composition was obtained using EDX on a Link ISIS X-ray energy-dispersive spectrophotometer with an ultrathin beryllium window.

Surface characterisation by X-ray photoelectron spectroscopy (XPS) was conducted on a Leybold–Heraeus LHS-10 spectrometer.

UV–vis spectra were recorded on a Varian Cary 5 spectrometer equipped with an integrating sphere using PTFE (polytetrafluoroethylene) as reference to study light absorption properties of the samples. Diffuse reflectance spectra were recorded and band gaps were calculated by the Kubelka–Munk function, according to the Tandon–Gupta method [9].

Phase composition, degree of crystallinity and crystal sizes were estimated from XRD patterns recorded on a PANalytical X´Pert diffractometer equipped with a Ni filter and Cu Kα radiation.

Size distribution of aggregates in aqueous suspension was analysed using a Mastersizer Hydro 2000 SM unit.

2.3. Experimental set-up

2.3.1. Physicochemical treatments

Different amounts of $WTiO_2$ were added to solutions of HFAs at 0.5 g L^{-1} (200 mL), to obtain concentrations in the range 0.25–2 g L^{-1}. These suspensions were stirred for 10 min (500 rpm) and subsequently left standing for 20 min until the precipitation ended. Ten millilitres of the supernatant were extracted for TOC and Fe determination to find the highest TOC reduction of the supernatant.

2.3.2. Advanced oxidation processes

The AOP employed involved the use of a borosilicate reactor, in this case a gas-washing bottle supplied by Alamo S.A., into which 200 mL of a 0.5 g L^{-1} solution of HFAs was poured. This organic matter concentration is equivalent to a 10-fold dilution of an old landfill leachate that consists mainly of humic and fulvic acids [10]. The light source was a Solarium Philips HB175 lamp equipped with four 15 W Philips CLEO fluorescent tubes. Emission spectrum was 300–400 nm with maximum peak at 365 nm. Stirring was performed with a stirring plate at 500 rpm and aeration with an air bubbler. In the photocatalysis studies, prior to illumination the suspensions were kept in the dark for 30 min to ensure adsorption equilibrium. Illumination of 2 h was used for all the studies and samples were taken every 30 min for TOC determination. In the case of photocatalysis, prior to the analysis the samples were filtered to eliminate the TiO_2 solids using 0.45-μm nitrocellulose filters. In the Fenton and

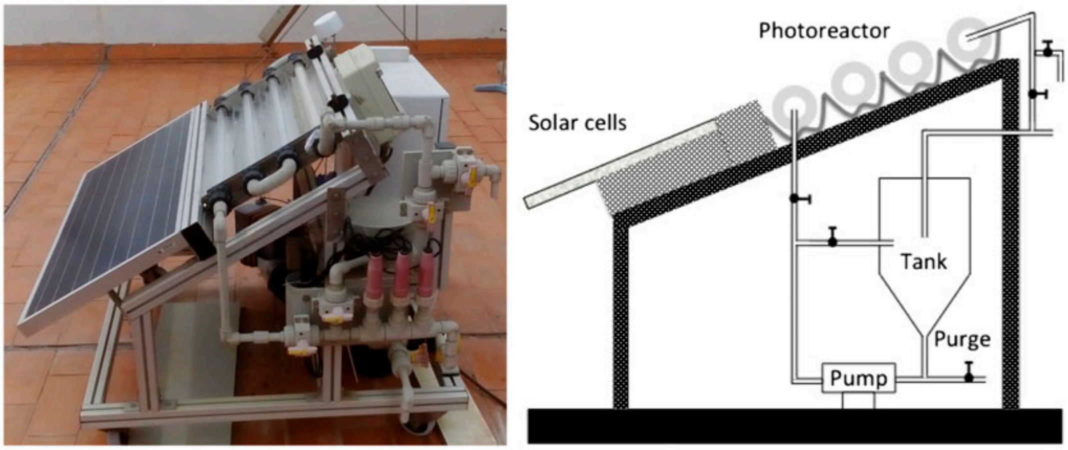

Fig. 1. (a) Photograph of the CPC solar photoreactor module and (b) hydraulic design of the CPC solar photoreactor module.

photo-Fenton processes, the total amount of H_2O_2 was added in equal amounts each 30 min for the 2 h of illumination.

The 5-L pilot plant (Fig. 1) was supplied by Ecosystem Environmental Services, S.A. It comprises a photoreactor (Solardetox Acadus-2010 Model, Ecosystem S.A.) consisting of a CPC (compound parabolic collector) module and four borosilicate glass tubes connected in series, a pump (Panworld 5PX-D) supplying a flow of 6 L min^{-1} and a UV-A radiometer (Acadus 85-PLS).

Table 1
Chemical composition (%wt.) of $WTiO_2$ from two production batches

%wt.	Ti	Fe	Si	Al
Sample 1	35.87	15.8	6.48	1.02
Sample 2	32.13	11.44	10.81	1.61
%wt.	Ca	Mg	K	Na
Sample 1	0.22	0.12	0.4	0.32
Sample 2	0.56	0.72	0.46	0.34

3. Results and discussion

3.1. Characterisation of $WTiO_2$

In Table 1, $WTiO_2$ composition is presented. Two analyses of two different batches are included in the Table, showing the stability in the chemical composition of the by-product generated in this industry. The main constituents are clearly Ti, Fe and Si, as the ilmenite is mostly comprised of oxides of iron and titanium, with appreciable amounts of amorphous silicate. XPS analysis reveals that Fe is in the trivalent state and the titanium in its tetravalent state [11].

The diffractograms of $WTiO_2$- and TiO_2-based photocatalyts are shown in Fig. 2(a). It is observed that $WTiO_2$ exhibits low crystallinity, although the main diffraction peaks of rutile and ilmenite phase are clearly seen. Though it is known that rutile phase is not the most photoactive phase of TiO_2 [12,13], surprising results have been seen for some kinds of compounds [14]. P25 and ECT consist of pure TiO_2 in two crystal phases, anatase and rutile, in ratios of 79:21 and 73:27, respectively. With regard to their optical properties, it is observed that the band gap of this waste material is lower than that of anatase and rutile and therefore lower than that of the P25 and ECT photocatalysts. This is because ilmenite is a wide band gap semiconductor with a value around 2.5 eV [15]. In addition and as expected due to its greenish colour, $WTiO_2$ absorbs radiation in the visible spectrum, (Fig. 2(b)).

Before its use in this study, the $WTiO_2$ was dried in a furnace at 105°C for two days and then subjected to grinding. The particle size distribution is shown in Fig. 3(a). A broad distribution with a maximum at 40 μm is observed.

When the material was suspended in water a shift was observed in the distribution of particles to larger sizes, indicating that significant particle aggregation takes place. The maximum of the distribution in this case corresponds to an aggregated value of 65 μm. Fig. 3(b) also presents an SEM image of the residue in which the heterogeneous particle size distribution and thin plate-like shapes are observed.

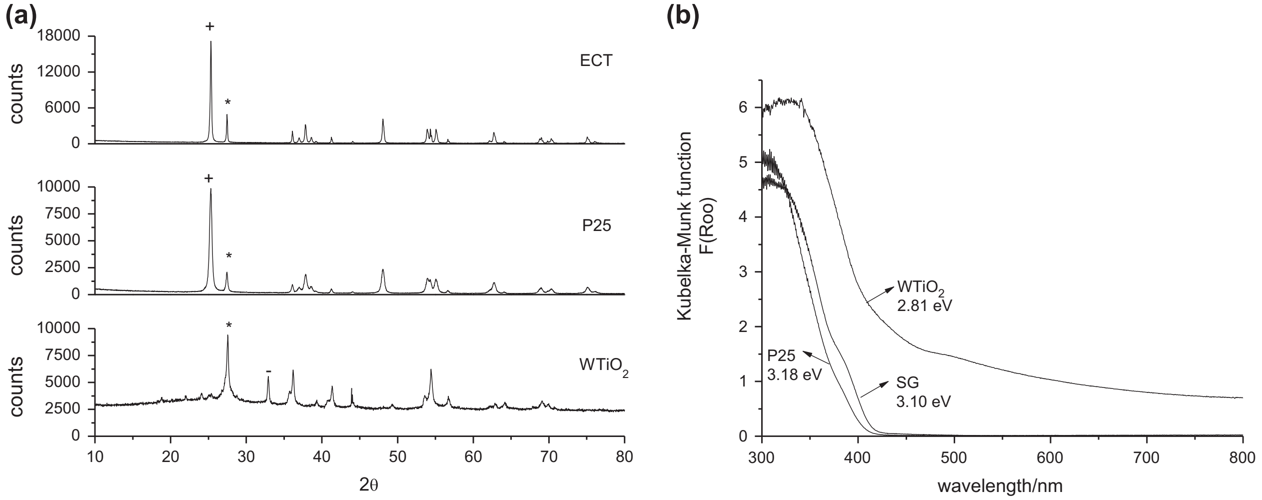

Fig. 2. (a) DRX patterns of the $WTiO_2$, P25 and ECT ((+) anatase, (*) rutile and (−) ilmenite) and (b) diffuse reflectance spectra.

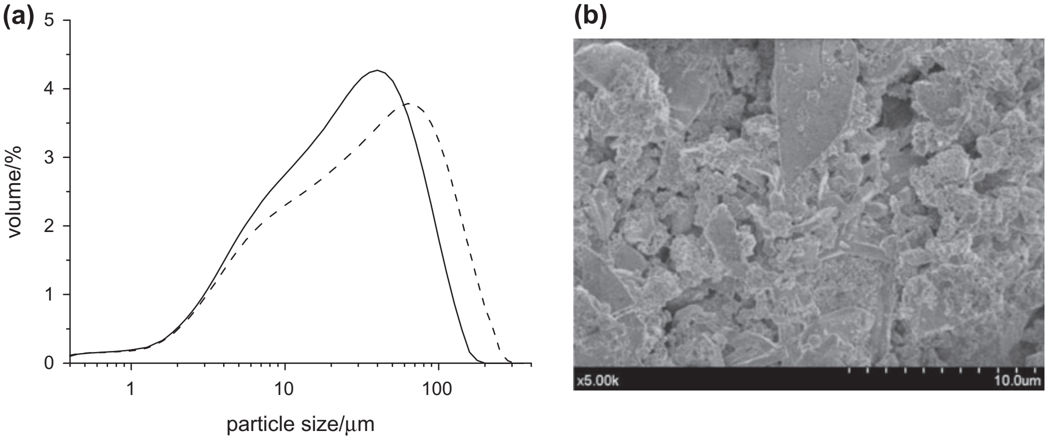

Fig. 3. (a) Size particle distribution of $WTiO_2$ in dry powder (solid line) and in aqueous suspension (dash line) and (b) SEM image of $WTiO_2$.

3.2. Preliminary studies

It was observed that the addition of $WTiO_2$ at a concentration of 1 g L^{-1} to a 0.5 g L^{-1} solution of HFAs resulted in a decrease from an initial pH of 9.5 to 3.0 and the immediate precipitation of a large amount of organic matter. The TOC of the resulting supernatant was reduced from 182.3 to 39.59 mg L^{-1} in 20 min. Though it might be supposed that this decrease in organic load could simply be due to the pH reduction (humic acids are not very soluble at low pH values), an additional coagulating effect of the Fe salts needs to be considered.

To determine the exact cause of this high level of precipitation when $WTiO_2$ was added, two HFAs solutions at 0.5 g L^{-1} were subjected to two different treatments. H_2SO_4 was added to one solution to adjust the pH to 3.0 and $FeCl_3$ to the other to obtain an Fe concentration equal to the Fe concentration obtained when 1 g L^{-1} of $WTiO_2$ was added to distilled water (44.29 mg L^{-1}). The results were compared with those obtained when the sample was treated with $WTiO_2$. It was noted that the addition of $FeCl_3$ ([Fe] = 44.29 mg L^{-1}) resulted in precipitation as fast as that produced by $WTiO_2$, although the percentage of TOC removed was slightly lower (78.7 vs. 82.3%). However, in the solution acidified with H_2SO_4 to pH 3.0 no significant precipitation was observed after 20 min, with a resulting TOC similar to that of the initial HFA solution. After 24 h, supernatant TOC was unchanged in both assays, suggesting that the effect of Fe on precipitation is immediate and that a pH of 3.0 is not adequate for precipitation of the humic acid fraction. A third assay performed at pH 2.0 showed TOC reduction after 24 h of only 20%. However, a fourth assay carried out at pH 1.0 resulted in a significant precipitation in 20 min, though 10% less than that obtained when Fe as $WTiO_2$ was added.

Fig. 4 shows the absorption spectra of the supernatant of the samples treated with $WTiO_2$, $FeCl_3$ and the addition of H_2SO_4 to pH 1.0. It can be observed that the absorption spectrum of the supernatant after addition of $FeCl_3$ is similar to that of the supernatant after precipitation with $WTiO_2$, with an absorption band appearing at 299 nm which is not observed in the case of H_2SO_4 addition. This absorption band is a consequence of the formation of humic acid–Fe complexes, as is described in the bibliography [16,17]. It was therefore concluded that the effect of the addition of $WTiO_2$ on organic matter precipitation was fundamentally due to coagulation through the soluble Fe components present in $WTiO_2$.

An extractive effect by HFAs was also observed of the Fe from the $WTiO_2$. Despite the Fe precipitating with the HFAs, an Fe concentration of 36.35 mg L^{-1} remained in solution when 1.0 g L^{-1} $WTiO_2$ was used, whereas in the case of the addition of $FeCl_3$ ([Fe] = 44.29 mg L^{-1}) only 4.19 ppm Fe remained in solution after precipitation.

Based on these preliminary studies, a treatment of HFA effluents is proposed consisting of two stages: first, a physical coagulation–flocculation process and, after filtration, a second step to treat the supernatant with an AOP.

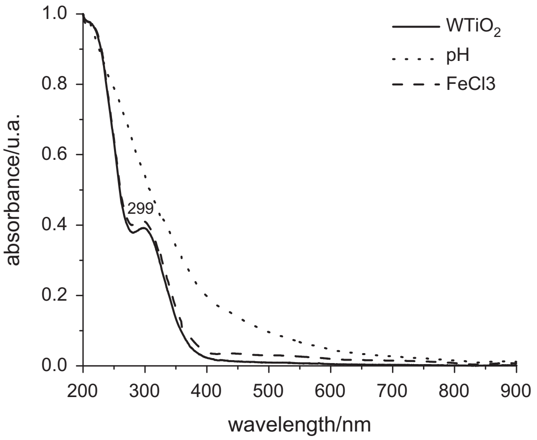

Fig. 4. Absorbance spectra of the supernatants resulting from the study of $WTiO_2$ addition (1 g L^{-1}), adjustment to pH 1 with H_2SO_4 and $FeCl_3$ ([Fe] = 44.29 mg L^{-1}) addition to an effluent containing 0.5 g L^{-1} HFAs.

3.3. Treatment

3.3.1. Coagulation–flocculation

The results of the physicochemical treatment of the HFA solutions (0.5 g L^{-1}) using $WTiO_2$ as coagulating agent (0.25–2 g L^{-1}) are shown in Table 2 and the effects of the treatment can be seen in Fig. 5.

At $WTiO_2$ concentrations lower than 0.5 g L^{-1}, the effect on the TOC value is insignificant. A sharp fall in TOC values can be observed when the $WTiO_2$ concentration is increased from 0.5 to 1 g L^{-1} after which TOC continues to decrease but at a much slower rate, reaching a value of 34.13 mg L^{-1} for 2.0 g L^{-1} of $WTiO_2$. This decrease is accompanied by a growing concentration of leached Fe from 6.69 to 66.37 mg L^{-1} for 2.0 g L^{-1} of $WTiO_2$. The pH values also were reduced as the $WTiO_2$ concentration was increased, with a value below pH 3.0 for concentrations at or above 1 g L^{-1}.

In short, based on the results of TOC reduction, 1.0 g L^{-1} is the optimum $WTiO_2$ concentration.

To study the potential reuse of $WTiO_2$, the precipitated residue ($WTiO_2$ + HFAs precipitate) was subjected to calcination at 450°C to eliminate the organic matter. Its subsequent addition to a new 0.5 g L^{-1} HFA solution did not result in any pH reduction and Fe leaching was insignificant (0.03 mg L^{-1}). Therefore, such results do not indicate potential reusability.

3.3.2. Advanced oxidation processes

The supernatant resulting from the application of a concentration of 1.0 g L^{-1} of $WTiO_2$ in 0.5 g L^{-1} of HFAs exhibits suitable characteristics for the application of the processes considered here (photocatalysis, Fenton and photo-Fenton), namely: (i) the system to be treated is sufficiently transparent for most of the active photons to reach the photocatalyst and to avoid interference such as scattering or absorption by other substances in suspension, and (ii) the residual amount of Fe that remains in solution and the natural pH of the process favour the photocatalytic degradation of HFAs, as this process is favoured at acid pH [18,19] similarly to Fenton and photo-Fenton processes. The only reagent that needs to be added in the latter processes is H_2O_2.

3.3.2.1. Photocatalysis. The photocatalytic activity of the $WTiO_2$ (1 g L^{-1}) on the supernatant obtained from the HFA solution (0.5 g L^{-1}) was compared with that of

Table 2
pH and concentrations of TOC and Fe of the supernatant resulting from the treatment of HFA solutions (0.5 g L^{-1}) with different concentrations of $WTiO_2$

$WTiO_2$/g L^{-1}	pH	Supernatant TOC/mg L^{-1}	[Fe]/mg L^{-1}
0.0	9.48	182.3	0.0
0.25	6.23	181.9	6.69
0.5	4.51	177.3	17.49
1.0	2.96	39.59	36.35
1.5	2.71	36.54	49.12
2.0	2.53	34.13	66.37

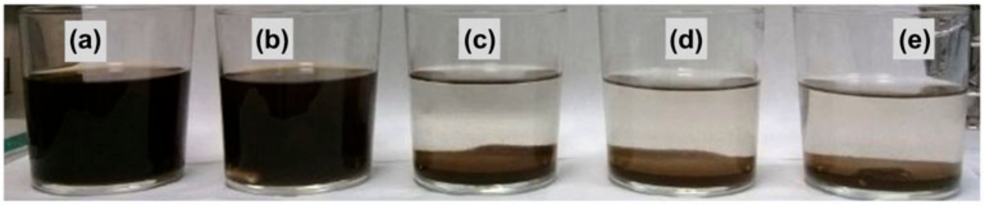

Fig. 5. View of the precipitation of an HFA solution (0.5 g L^{-1}) with different concentrations of $WTiO_2$ added for 20 min of sedimentation: (a) 0.25 g L^{-1}, (b) 0.5 g L^{-1}, (c) 1 g L^{-1}, (d) 1.5 g L^{-1} and (e) 2 g L^{-1}.

other TiO_2-based materials at the same concentration (1 g L^{-1}). These were P25, which has displayed high activity for a large number of pollutants and which is used as a reference material in photocatalytic studies of new materials [20,21], and ECT, which in previous studies has displayed high levels of activity that are comparable in many cases to that of P25 [6,7]. As can be seen in Fig. 6, none of the materials used as catalysts produced significant TOC removal in HFA degradation after 30 min in darkness. In the presence of light, the $WTiO_2$ and P25 displayed very low photocatalytic activity, with 93 and 81%, respectively, of initial TOC remaining in solution. However, the ECT photocatalyst did achieve evident mineralisation, with 51% of initial TOC remaining in solution after 2 h of illumination. $WTiO_2$ was tested at concentrations lower and higher than 1 g L^{-1}, namely 0.5 and 2 g L^{-1}, and no activity was observed. 0.5 g L^{-1} seems to be insufficient to show activity and in 2 g L^{-1} the active surface area is reduced due to catalyst particle aggregation and radiation scattering is favoured impeding the transmission of the radiation throughout the photoreactor with the result that it does not reach the active centres of the catalyst particles [22–24]. The $WTiO_2$ was also subjected to different calcination temperatures with no photoactivity subsequently observed (results not shown). In view of the results, it was concluded that $WTiO_2$ is inactive in terms of photocatalytic degradation of HFAs and, moreover, that photocatalysis in general does not appear to be a suitable treatment for HFA effluent.

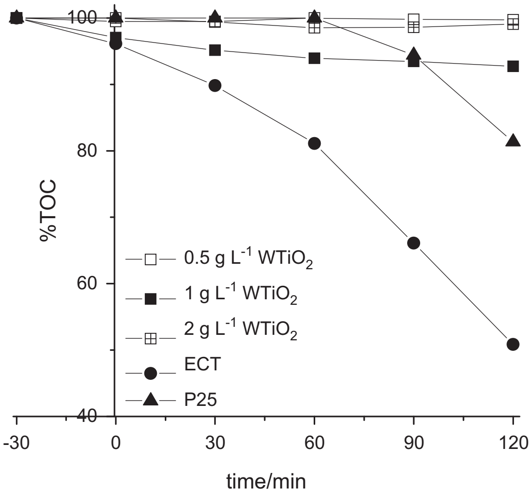

Fig. 6. Mineralisation achieved by the photocatalytic degradation with $WTiO_2$, ECT and P25 of the supernatant produced in the flocculation treatment of the HFA effluent.

3.3.2.2. *Fenton and photo-Fenton.* Taking into account that the Fe concentration in the supernatant of the HFA solution (0.5 g L^{-1}) with 1.0 g L^{-1} of $WTiO_2$ was

36.35 mg L^{-1}, the concentration of H_2O_2 necessary for the photo-Fenton process was optimised using different molar ratios $[H_2O_2]/[Fe]$: 8, 10, 13 and 18. The resulting amount of H_2O_2 was not added all at once at the beginning of the process but in four equal doses, each at 30 min intervals for the two hours of the test. This was done following the recommendations of Tseng et al. [25], with the aim of avoiding the adverse effects of high concentrations of H_2O_2 such as the capture of $HO^{\cdot}$ radicals and competition with the pollutant for adsorption centres [26]. Fig. 7(a) shows the corresponding mineralisation results for the photo-Fenton process at the different $[H_2O_2]/[Fe]$ ratios and, for purposes of comparison, the Fenton process for the ratio $[H_2O_2]/[Fe] = 8$.

As can be seen, the photo-Fenton process was effective in terms of supernatant degradation compared with the results obtained by photocatalysis and by the Fenton process. After 120 min, the lowest removal yields were obtained at a ratio $[H_2O_2]/[Fe] = 8$ for the Fenton (13.1%) and photo-Fenton (56.9%) processes. When the ratio was increased to 10, the photo-Fenton mineralisation rose sharply, reaching a removal rate of 81.3%. At higher $[H_2O_2]/[Fe]$ ratios, TOC removal continued to increase, though more smoothly, reaching 91.3% for a ratio of 18.

The residual concentration of H_2O_2, that is the H_2O_2 remaining at the end of the process which consequently had not contributed to mineralisation, was also measured (Fig. 7(b)). As can be seen, in the Fenton process, despite a TOC reduction much lower than that obtained in the photo-Fenton process, the concentration of H_2O_2 was considerably reduced. This is due to the inherent instability of this reagent which also contributes to making a split-dosing process more effective than adding the H_2O_2 in one go at the beginning.

In the photo-Fenton process at a ratio $[H_2O_2]/[Fe] = 10$, the concentration of residual H_2O_2 was very similar to that obtained with a ratio of 8 (2.04 vs. 2.79 mg L^{-1}). Nonetheless, this concentration rose sharply at higher ratios attaining a value of 10.85 mg L^{-1} for a ratio of 13 without any significant further reduction in TOC. This led us to take a ratio of 10 as the optimum ratio for the photo-Fenton process. In short, the overall TOC removal, taking into consideration the two stages of coagulation–flocculation and photo-Fenton, was 95.9%.

The mechanism for the photo-Fenton process applied to HFA effluent has been described in the literature [16]. A ligand–metal charge transfer occurs photoinduced in the Fe(III)–HFA complex through the effect of light:

$$\mathrm{Fe(III)} - \mathrm{HFA_{red}} \xrightarrow{\text{light}} \mathrm{Fe(II)} - \mathrm{HFA_{ox}} \tag{5}$$

and the Fe(II) is reoxidised by the H_2O_2 generating hydroxyl radicals in accordance with the following equation:

$$\mathrm{Fe^{2+}} + \mathrm{H_2O_2} \xrightarrow{\text{light}} \mathrm{Fe^{3+}} + \mathrm{HO^-} + \mathrm{HO^{\cdot}} \tag{6}$$

These radicals attack the organic matter until its complete mineralisation. The Fe(III) can also be reduced to Fe(II) through the typical reaction of the photo-Fenton process:

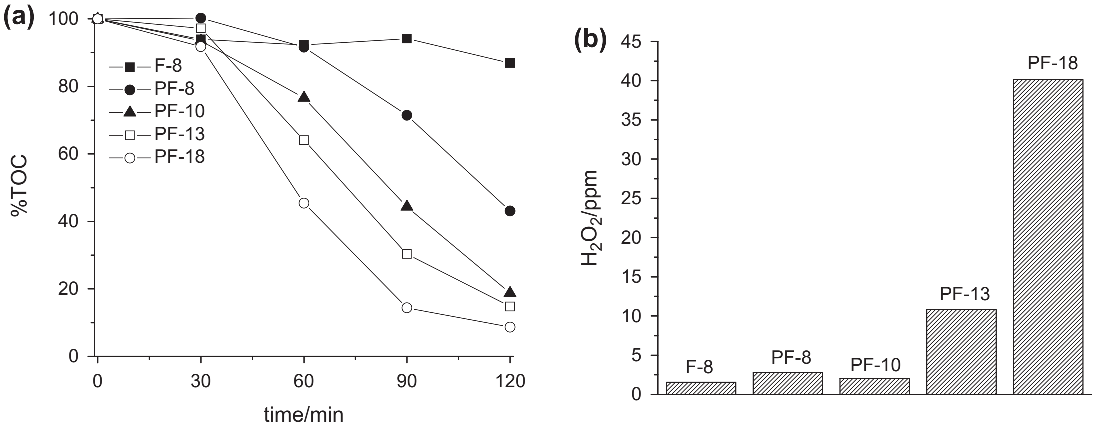

Fig. 7. (a) Mineralisation achieved by the Fenton and photo-Fenton processes of the supernatant produced in the treatment of the HFA effluent, at different $[H_2O_2]/[Fe]$ ratios and (b) concentration of the residual H_2O_2 (F indicates Fenton, PF indicates photo-Fenton and the number indicates the ratio $[H_2O_2]/[Fe]$).

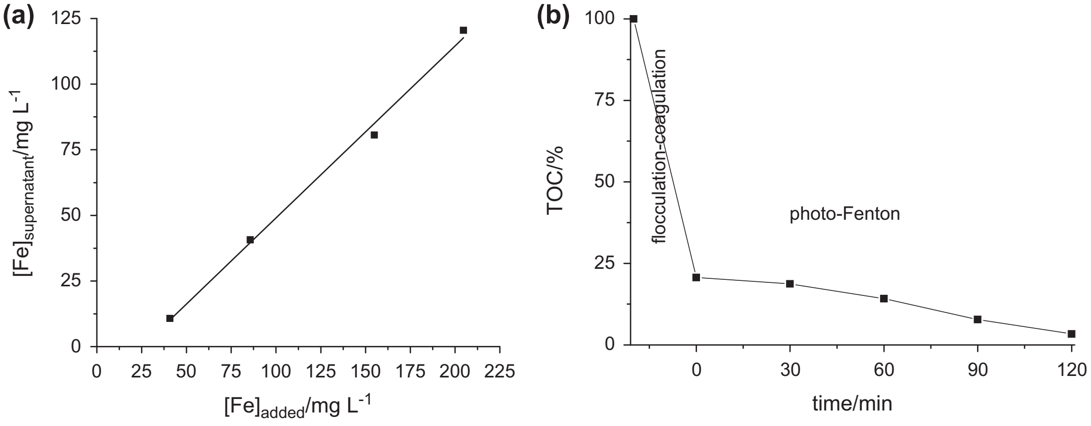

Fig. 8. (a) Fe concentration remaining in solution (supernatant) vs. Fe concentration added as $FeCl_3·6H_2O$ to a 0.5 g L^{-1} HFA solution and (b) treatment of a 0.5 g L^{-1} HFA solution with $FeCl_3·6H_2O$ ([Fe] = 84.85 mg L^{-1}).

$$Fe^{3+} + H_2O \xrightarrow{\text{light}} Fe^{2+} + H^+ + HO^{\cdot} \qquad (7)$$

Toxicity tests were conducted as the final step of this study. Toxicity was measured in the initial solution of 0.5 g L^{-1} of HFAs filtered through 0.45-μm nitrocellulose filters, in the supernatant obtained after the coagulation–flocculation stage with the addition of 1 g L^{-1} $WTiO_2$ and in the sample at the end of the optimised photo-Fenton process. Positive toxicity results were only found in the initial solution, with an inhibition percentage of 14.7%, and this problem was therefore eliminated after the first stage of the process. It was also observed that the intermediates that were generated and the residual H_2O_2 did not introduce any additional toxicity, and so the addition of catalase or any other system to eliminate the latter was not necessary.

3.4. Fe elimination

At the end of the treatments with $WTiO_2$, the remaining Fe becomes a residue that needs to be removed in order to meet regulatory limits (10 mg L^{-1} in accordance with Spanish Royal Decree 849/1986, dated 11th April).

If removal of the Fe remaining after the treatment with $WTiO_2$ is considered of interest, the simplest and the most effective method is its removal by precipitation in hydroxide form, increasing the effluent pH with NaOH [27]. Thus, it was noted that a small increase in pH from 3 to 4.65 obtained a reduction in Fe concentration to a final value of 2.33 mg L^{-1} and that this could be even further reduced at higher pH values, with an Fe concentration of less than 0.1 mg L^{-1} at pH 6.70. In short, a slight increase in pH resulted in the Fe concentration falling below the maximum permissible amount.

3.5. Fe(III) from commercial reactive

For purposes of comparison of $WTiO_2$ with an equivalent commercial product, a series of tests were conducted at laboratory scale using $FeCl_3$.

Firstly, it was necessary to find the amount of $FeCl_3$ that has to be added to the initial effluent so that after coagulation–flocculation 36.35 ppm Fe still remained in the supernatant to be treated by photo-Fenton. Increasing amounts of $FeCl_3$ were added to different 0.5 g L^{-1} HFA solutions. Fe concentration remaining in the supernatant was measured after 20 min and a linear trend was observed between $[Fe]_{supernatant}$ and $[Fe]_{added}$ (Fig. 8(a)). The regression equation allows to determine that the effect of 1.0 g L^{-1} of $WTiO_2$ ($[Fe]_{supernatant}$ = 36.35 mg L^{-1}) corresponded to the addition of an Fe concentration of 84.85 mg L^{-1}.

The results of the treatment of 0.5 g L^{-1} HFA solution with the amount of $FeCl_3$ that supplies 84.85 mg L^{-1} Fe were similar to those for the $WTiO_2$ in both treatment stages (coagulation–flocculation and photo-Fenton), as can be seen in Fig. 8(b). The amount of remaining hydrogen peroxide was also similar with a value of 2.31 ppm.

3.6. Pilot plant studies

Fig. 9 shows the mineralisation of a 0.5 g L^{-1} HFA solution obtained in the previously described two-stage treatment when implemented at pilot plant scale.

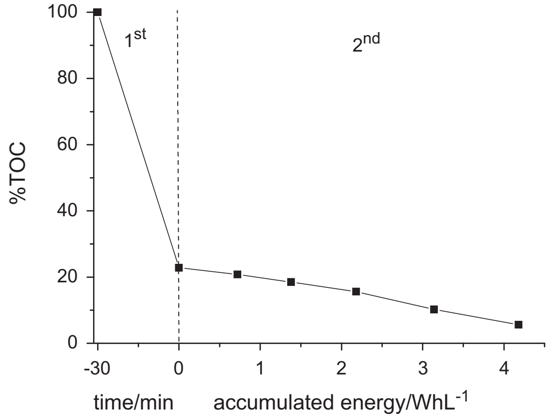

Fig. 9. Mineralisation achieved applying the proposed two-stage process at pilot plant scale to: (■) HFAs at 0.5 g L^{-1} ($[H_2O_2]/[Fe]$ = 10).

The two stages (coagulation–flocculation and photo-Fenton processes) were developed under the optimised conditions obtained at laboratory scale. For the first stage, 5 L of solution were treated with 1 g L^{-1} of $WTiO_2$. For the second stage, as in the laboratory tests, the H_2O_2 was added to the supernatant in equal doses each 30 min to obtain an overall ratio $[H_2O_2]/[Fe]$ = 10.

As can be seen, 77.2% of TOC removal was attained in the first stage. In the second stage, with an accumulated energy of 4.10 Wh L^{-1}, a further 17.2% of mineralisation yielded an overall TOC removal of 94.4%. Therefore, these results are similar to those obtained at laboratory scale. Moreover, the final solution was verified to be non-toxic, the concentration of residual H_2O_2 was low (0.95 mg L^{-1}) and Fe concentration was reduced to below the maximum legal limits by slightly increasing the pH, with 3.35 mg L^{-1} obtained at pH 4.76.

4. Conclusions

This study investigated the potential reuse of a waste material from the TiO_2 pigment manufacturing industry. Though $WTiO_2$ did not display an appreciable photocatalytic activity in the treatment of a 0.5 g L^{-1} solution of HFAs, its use could be exploited in other AOPs such as photo-Fenton. Part of the Fe, which is one of the components of $WTiO_2$, is leached into the solution and contributes to the precipitation of the HFAs. In addition, a sufficient amount of Fe remains in solution to carry out a photo-Fenton process. A possible two-stage treatment for landfill leachate is therefore suggested: an initial stage of coagulation–flocculation–precipitation and a second stage involving the photo-Fenton process. The optimum $[H_2O_2]/[Fe]$ molar ratio for the photo-Fenton process was found to be 10. With the combined two-stage process, overall TOC removal amounted to 95.9% and the resulting solution is non-toxic. The process was scaled to a volume of 5 L in a small-scale pilot plant and the results obtained were concordant with those obtained at laboratory scale for both stages. Overall TOC removal was higher than 90% for 4.10 Wh L^{-1} of accumulated energy.

Acknowledgements

The authors acknowledge the financial support for this research from the Spanish Ministry of Science and Innovation (MICINN) under the project FOXMORE (CTM2006-05114) and from the Spanish Ministry of Economy and Competitiveness under the Infrastructure Project UNLP10-3E-726, co-financed with ERDF funds. E. Pulido Melián would also like to thank the University of Las Palmas de Gran Canaria for her postdoctoral contract.

References

[1] C. Sasikumar, D.S. Rao, S. Srikanth, N.K. Mukhopadhyay, S.P. Mehrotra, Dissolution studies of mechanically activated Manavalakurichi ilmenite with HCl and H_2SO_4, Hydrometallurgy 88 (2007) 154–169.

[2] C.B. Öman, C. Junestedt, Chemical characterization of landfill leachates-400 parameters and compounds, Waste Manage. 28 (2008) 1876–1891.

[3] S.Q. Aziz, H.A. Aziz, M.S. Yusoff, M.J.K. Bashir, Leachate characterization in semi-aerobic and anaerobic sanitary landfills: A comparative study, J. Environ. Manage. 91 (2010) 2608–2614.

[4] E.M.R. Rocha, V.J.P. Vilar, A. Fonseca, I. Saraiva, R.A.R. Boaventura, Landfill leachate treatment by solar-driven AOPs, Sol. Energy 85 (2011) 46–56.

[5] M. Steiner, U. Wiegel, The Book of Rubbish: European Leonardo Da Vinci Project-Waste Training; A Guide to the Basics of Waste Management, Sunny Area Publishers, Turkey, 2008.

[6] J. Araña, J.M. Doña Rodríguez, D. Portillo Carrizo, C. Fernández Rodríguez, J. Pérez Peña, O. González Díaz, J.A. Navío, M. Macías, Photocatalytic degradation of phenolic compounds with new TiO_2 catalysts, Appl. Catal. B: Environ. 100 (2010) 346–354.

[7] E.I. Seck, J.M. Doña Rodríguez, C. Fernández Rodríguez, O. González Díaz, J. Araña, J. Pérez Peña, Photocatalytic removal of 2,4-dichlorophenoxyacetic acid by using sol–gel synthesized nanocrystalline and commercial TiO_2: Operational parameters optimization and toxicity studies, Appl. Catal. B: Environ. 125 (2012) 28–34.

[8] R.M. Sellers, Spectrophotometric determination of hydrogen peroxide using potassium titanium(IV) oxalate, The Analyst 105 (1980) 950–954.

[9] S.P. Tandon, J.P. Gupta, Measurement of forbidden energy gap of semiconductors by diffuse reflectance technique, Phys. Status Solidi B 38 (1970) 363–367.

[10] H. Ngo, W. Guo, W. Xing, Applied technologies in munipal solid waste landfil lechate treatment, in: S. Vigneswaran (Ed.), Water and Wastewater treatment technologies, in: Encyclopedia of Life Support Systems (EOLSS), Eolss Publishers, Paris, France, Developed under the Auspices of the UNESCO, 2008.

[11] L.F. Vilches, C. Fernández-Pereira, J. Olivares, J. Vale, Recycling potential of coal fly ash and titanium waste as new fireproof products, Chem. Eng. J. 95 (2013) 155–161.

[12] T. Luttrell, S. Halpegamage, J. Tao, A. Kramer, E. Sutter, M. Batzill, Why is anatase a better photocatalyst than rutile?—Model studies on epitaxial TiO_2 films, Sci. Rep. 4 (2014) 1–8.

[13] Q. Sun, Y. Xu, Evaluating intrinsic photocatalytic activities of anatase and rutile TiO_2 for organic degradation in water, J. Phys. Chem. C 114 (2010) 18911–18918.

[14] J. Ryu, W. Choi, Substrate-specific photocatalytic activities of TiO_2 and multiactivity test for water treatment application, Environ. Sci. Technol. 42 (2008) 294–300.

[15] R. Wilkins, K.S.A. Powell, Characterizing surfaces of the wide bandgap semiconductor ilmenite with scanning probe microcopies, NASA University Research Centers Technical Advances in Education, Aeronautics, Space, Autonomy, Earth and Environment Conference Paper (SEE 20010000359), 1, (1997) 797–801.

[16] M. Fukushima, K. Tatsumi, Photocatalytic reaction by iron(III)-humate complex and its effect on the removal of organic pollutant, Toxicol. Environ. Chem. 73 (1999) 103–116.

[17] A. Georgi, A. Schierz, U. Trommler, C.P. Horwitz, T.J. Collins, F.D. Kopinke, Humic acid modified Fenton reagent for enhancement of the working pH range, Appl. Catal. B: Environ. 72 (2007) 26–36.

[18] Z. Yigit, H. Inan, A study of the photocatalytic oxidation of humic acid on anatase and mixed-phase anatase–rutile TiO_2 nanoparticles, Water Air Soil Pollut. Focus 9 (2009) 237–243.

[19] J. Wiszniowski, D. Robert, J. Surmacz-Gorska, K. Miksch, J.V. Weber, Photocatalytic mineralization of humic acids with TiO_2: Effect of pH, sulfate and chloride anions, Int. J. Photoenergy 5 (2003) 69–74.

[20] E. Pulido Melián, O. González Díaz, J.M. Doña Rodríguez, G. Colón, J.A. Navío, J. Pérez Peña, Effect of hydrothermal treatment on structural and photocatalytic properties of TiO_2 synthesized by sol-gel method, Appl. Catal. A: Gen. 411–412 (2012) 153–159.

[21] E. Pulido Melián, O. González Díaz, A. Ortega Méndez, C.R. López, M.N. Suárez, J.M. Doña Rodríguez, J.A. Navío, D. Fernández Hevia, J. Pérez Peña, Efficient and affordable hydrogen production by water photo-splitting using TiO2-based photocatalysts, Int. J. Hydrogen Energy 38 (2013) 2144–2155.

[22] P. Chowdhury, G. Malekshoar, M.B. Ray, J. Zhu, A.K. Ray, Sacrificial hydrogen generation form formaldehyde with Pt/TiO_2 photocatalyst in solar radiation, Ind. Eng. Chem. Res. 52 (2013) 5023–5029.

[23] E. Pulido Melián, O. González Díaz, J.M. Doña Rodríguez, J. Araña, J. Pérez Peña, Adsorption and photocatalytic degradation of 2,4-dichlorophenol in TiO_2 suspension. Effect of hydrogen peroxide, sodium peroxodisulphate and ozone, Appl. Catal. A: Gen. 455 (2013) 227–233.

[24] S. Kaur, V. Singh, TiO_2 mediated photocatalytic degradation studies of Reactive Red 198 by UV irradiation, J. Hazard. Mater. 141 (2007) 230–236.

[25] D.H. Tseng, L.C. Juang, H.H. Huang, Effect of oxygen and hydrogen peroxide on the photocatalytic degradation of monochlorobenzene in TiO_2 aqueous Suspension, Int. J. Photoenergy. 2012 (2012) 9 pages, ID 328526, doi: 10.1155/2012/328526.

[26] S. Malato, J. Blanco, C. Richter, B. Braun, M.I. Maldonado, Enhancement of the rate of solar photocatalytic mineralization of organic pollutants by inorganic oxidizing species, Appl. Catal. B: Environ. 17 (1998) 347–356.

[27] D.E. Santiago, J. Araña, O. González Díaz, E. Henríquez Cárdenes, J.A. Ortega Méndez, E. Pulido Melián, J.M. Doña-Rodríguez, J. Pérez-Peña, Treatment of wastewater containing imazalil by means of Fenton-based processes, Desalin. Water Treat. 57 (2016) 13865–13877, doi: 10.1080/19443994.2015.1061452.